Fluctuations in productivity and denitrification in the southeastern Arabian Sea during the Late Quaternary

Pratima M. Kessarkar[1,*], V. Purnachandra Rao[1], S. W. A. Naqvi[1], Allan R. Chivas[2] and T. Saino[3]

[1]National Institute of Oceanography, Council of Scientific and Industrial Research, Dona Paula, Goa 403 004, India
[2]Geo-QuEST Research Centre, School of Earth and Environmental Sciences, University of Wollongong, NSW 2522, Australia
[3]Hydrospheric Atmospheric Research Center, Nagoya University, Furo-cho, Chikusa-ku, Nagoya 464-8601, Japan

Sedimentological and stable isotopic characteristics of sediments have been studied in a core from the southeastern Arabian Sea containing records of the past 70 ka. Palaeoproductivity proxies such as organic carbon (C_{org}), total nitrogen (TN) and calcium carbonate ($CaCO_3$) contents, show high values at the core top and during the Last Glacial Maximum (LGM) and marine isotope stage (MIS) 4, suggesting high productivity, whereas low C_{org} and $CaCO_3$ contents are associated with the MIS 1/2 and mid-MIS 3, indicating reduced productivity. The $\delta^{18}O$ values in planktonic foraminifera range between – 2.7‰ and – 0.1‰, with a large glacial–interglacial amplitude $\Delta\delta^{18}O$ of ~ 2.6‰, suggesting changes related to monsoonal precipitation/runoff. The $\delta^{15}N$ values fluctuate between 5.4‰ and 7.3‰, signifying variation in denitrification intensity. The $\delta^{15}N$ indicates an overall increase in denitrification intensity during MIS 1 and MIS 3 and, reduced intensity during MIS 1/2, LGM and mid-MIS 3. Higher primary productivity and reduced denitrification intensity during LGM and MIS 4 might be due to convective winter mixing and more oxygenated subsurface waters. Reduced primary productivity during MIS 1/2 and mid-MIS 3 might be the effect of enhanced precipitation associated with the intensified southwest monsoon fortifying near-surface stratification.

Keywords: Arabian Sea, denitrification, productivity, stable isotopes.

THE Arabian Sea is one of the most productive regions of the world ocean, marked by large-scale water-column denitrification, which also occurs in the eastern tropical North and South Pacific[1]. Denitrification is considered to be a major sink for oceanic fixed nitrogen that controls the oceanic nitrate inventory, in turn influencing global primary productivity and CO_2 sequestration by the biological pump[2]. The Arabian Sea also serves as an important source of N_2O, a potent greenhouse gas[3]. It is well accepted that the high $\delta^{15}N$ values in intermediate waters and particulate organic matter in this region are the result of denitrification linked to the intensity of the summer monsoon and associated upwelling and productivity[4,5]. The basin-wide homogenization of the $\delta^{15}N$ signal is related to the circulation pattern in the Arabian Sea[6]. Temporal changes in the intensity of denitrification in the Arabian Sea have been linked to fluctuations in atmospheric N_2O on glacial–interglacial scales[7]. The organic carbon (C_{org}) accumulation in the sediments has been used as a productivity proxy driven by the intensity of the southwest monsoon in the past[8]. Several workers have reported C_{org} variations during glacial and interglacial times in the Arabian Sea and related them to changes in water masses, productivity and climate, both on regional and global scales[9–12]. Past variations in monsoon-induced denitrification intensity suggest a link between the climates of the Arabian Sea and the North Atlantic[13]. Reduced denitrification as a result of better ventilation of mid-water during the Younger Dryas and Heinrich events is related to oceanic teleconnection with water masses advecting from the south[13]. Most of the studies in the Arabian Sea have been concentrated in its northern and western regions, where high productivity occurs during both the northeast and southwest monsoons (see Figure 1). We have chosen a core (SK126/39) from the southeastern Arabian Sea that experiences upwelling-induced productivity only during the southwest monsoon, and is located close to the boundary of the perennial denitrification zone (Figure 1). This is one of the most suitable sites to track variations in the southwest monsoon-related productivity and intensity of denitrification. The purpose of this article is to understand fluctuations in marine productivity and intensity of denitrification during the Late Quaternary and Holocene.

Oceanographic conditions in the study area

The Arabian Sea experiences reversals in atmospheric and surface oceanic circulation associated with the

*For correspondence. (e-mail: pratimak@nio.org)

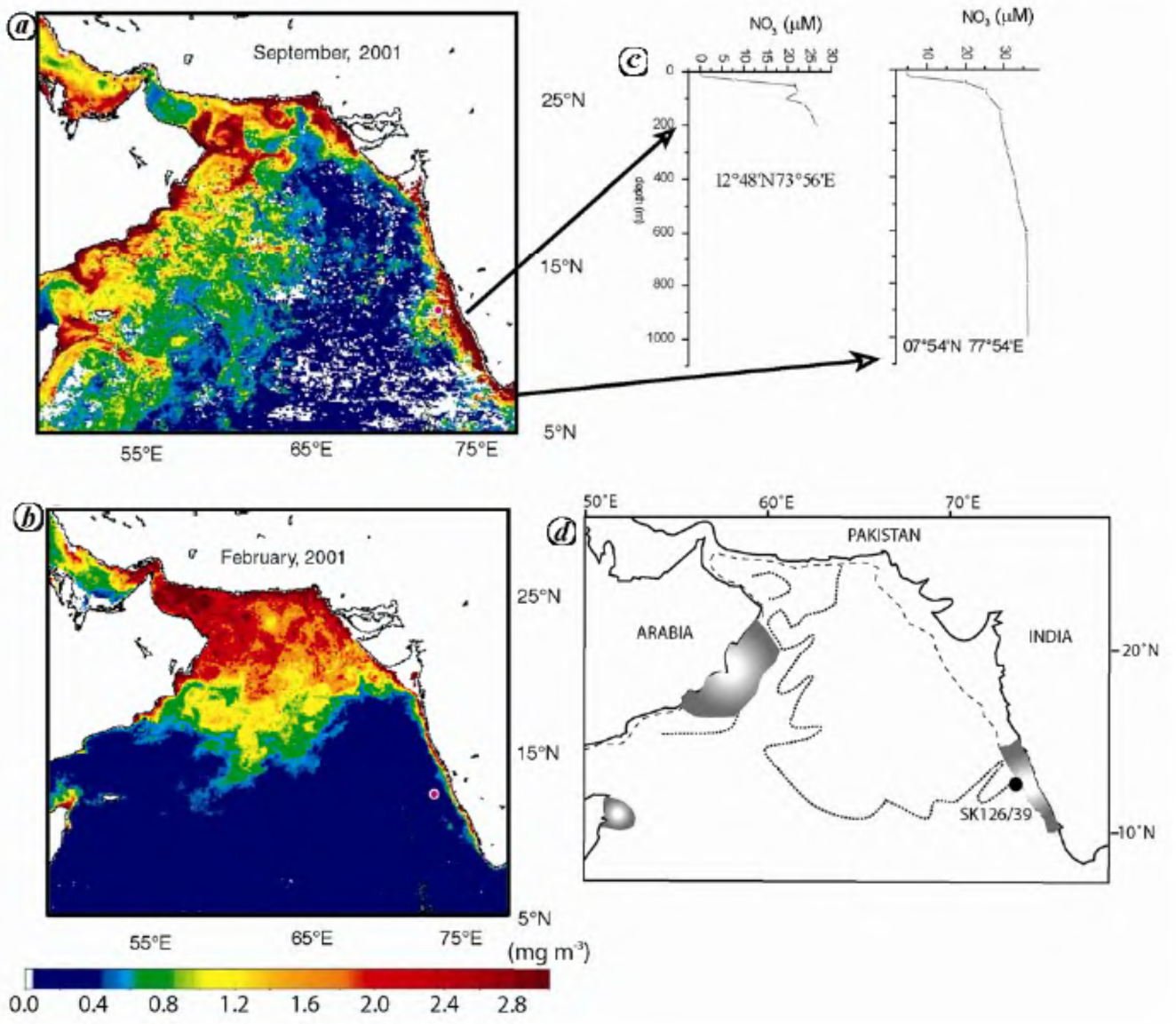

Figure 1. ***a*** and ***b***, Core location (marked in pink circle) on satellite imageries of the Arabian Sea indicating distribution of chlorophyll *a*. Red colour indicates high productivity during (***a***) southwest monsoon and (***b***) northeast monsoon. ***c***, Water column profiles of NO_3 content. ***d***, Location of the gravity cores with respect to the denitrification zone (marked in grey dotted line) and high productivity area with grey shade (modified after Naqvi[1]; Quasim[14], and Naqvi *et al.*[17]).

southwest and northeast monsoons. Winds and surface currents during the southwest monsoon are conducive for upwelling of nutrient-rich subsurface waters, giving rise to high productivity off Arabia, Somalia and southwestern India[14] (Figure 1 *a*). Increased productivity is also observed during the northeast monsoon due to convective mixing north of about 15°N (Figure 1 *b*). These phenomena make the Arabian Sea one of the most productive areas of the world ocean. The subsurface water renewal in the Indian Ocean mostly occurs through advection of waters from the south and locally formed intermediate waters (outflows from the Persian Gulf and Red Sea) in the northwestern region. As the renewal rate of water is moderate and productivity is high, a pronounced perennial oxygen minimum zone (OMZ) with dissolved $O_2 < 0.5$ ml l^{-1} (~22 μM) has developed in the Arabian Sea at water depths between 150 and 1200 m (refs 15 and 16). The acute oxygen deficiency leads to large scale denitrification in the water column within a zone that extends from the continental margin off Gujarat to the central Arabian Sea[1,17] (see Figure 1). Core SK126/39 lies within the high productivity area but at the boundary of this zone (Figure 1). The nitrate profile taken close to the study area exhibits a slight minimum at 100 m depth (Figure 1 *c*) presumably due to denitrification, whereas further south (e.g. at 7°S), high nitrate concentrations persist throughout the subsurface water column (Figure 1 *c*), suggesting an absence of denitrifying conditions.

Methods

We have analysed a 70 k year record of southwest monsoon variability from 490 cm long gravity core collected during the 126th cruise of *ORV Sagar Kanya* (SK126/39). The core SK126/39 was recovered from 12.63°N; 73.33°E, 1940 m water depth in the southeastern Arabian Sea (Figure 1). Sub-sampling of the core was done onboard at 2 cm intervals in the top 20 cm and 5 cm intervals in the rest of the core. The calcium carbonate ($CaCO_3$) content of the bulk sediments was determined by rapid gasometric technique, with reproducibility better than ± 5%. C_{org} and total nitrogen (TN) contents were determined using an elemental analyser (NCS 2500), with reproducibility of ± 1% for C_{org}. Nitrogen isotopic analysis was carried out on carbonate-free samples in a Carlo Erba NA2500NC elemental analyser coupled to a Finnigan MAT 252 isotope ratio mass spectrometer at the Hydrospheric–Atmospheric Research Center (Institute for Hydrospheric–Atmospheric Science), Nagoya University, Nagoya, Japan. The $\delta^{15}N$ value is expressed in per mille (‰) relative to atmospheric N_2. The analytical precision based on replicates of laboratory standards was about ± 0.2‰ for $\delta^{15}N$. About 15–20 tests of *Globigerinoides ruber* in the size range of 250–350 μm were hand picked under a binocular microscope from each level and analysed for oxygen isotopes using a MultiPrep (acid on individual carbonate at 90°C) unit attached to a PRISM III mass spectrometer calibrated against the NBS 18 and NBS 19 standards with analytical conditions as described by Chivas *et al.*[18], at the School of Earth and Environmental Sciences, University of Wollongong, Australia. The isotopic ratios are reported in standard delta notations with respect to Vienna Pee Dee Belemnite (V-PDB). Repeated analysis of standards indicated internal reproducibility of <0.1‰. The average sampling resolution for the oxygen isotopes is about 0.9 kilo annum (ka) for marine isotope stage (MIS) 1 and 2, and 1.6 ka for MIS 3 and 4.

Chronostratigraphy for each core is based on three radiocarbon measurements on *G. ruber* at the Leibniz-Labor of University of Kiel, Germany, using accelerator mass spectrometry (AMS) and, two bulk sample measurements by conventional radiocarbon method at the Birbal Sahni Institute of Palaeobotany, Lucknow, India. The bulk carbonate ages are generally higher due to the presence of old carbonates. The measured ages are after Kessarkar[19] calibrated using CALIB 4.3 program of Stuiver *et al.*[20].

Results

Stratigraphy

An age model was obtained by using calibrated ^{14}C dates[19] as control points and linearly interpolating the ages between the control points. The ages of sediment layers older than the ^{14}C ages were obtained by assigning tie points by correlating $\delta^{18}O$ curves with the stacked SPECMAP $\delta^{18}O$ curve[21,22]. We have linearly interpolated ages between these tie points and used these to calculate sedimentation rates (Figure 2). The core records for the past 70 ka going back to MIS 4, with the interpolated sedimentation rates varied between 6 and 8 cm/ka.

Variations in $\delta^{18}O$

The $\delta^{18}O$ values of *G. ruber* in the core vary between -2.7‰ and -0.1‰ (Figure 3). The core top represents the Holocene, marked by lower $\delta^{18}O$ values of -2.5‰ whereas higher $\delta^{18}O$ values are found ~ 22 ka before present (BP). The glacial–interglacial amplitude, $\Delta\delta^{18}O$ (the difference between peak glacial and interglacial $\delta^{18}O$ values) is ~ 2.6‰, with residual $\Delta\delta^{18}O$ ($\Delta\delta^{18}O$ after subtracting combined global ice volume effect and regional deglacial warming) of ~ 0.9‰. The $\delta^{18}O$ values are lower during interglacials and higher during glacial intervals. Low $\delta^{18}O$ values (-1.4‰ to -0.2‰) occur during MIS 3 with maximum depletion at ~ 40 ka BP (-1.3‰) and ~ 50 ka BP (-1.4‰). The $\delta^{18}O$ of ~ -0.7‰ is the highest value observed during MIS 4.

$CaCO_3$, C_{org} and TN

The $CaCO_3$ content ranges between 16% and 30% with overall lowest during MIS 2 and MIS 4 and highest during MIS 1 and MIS 3 (Figure 3). Prominent low $CaCO_3$ contents occur at the MIS 1/2 boundary (~ 11 to 9 ka BP) and mid-MIS 3 (~ 40 and ~ 50 ka BP). The C_{org} content varies between 0.8% and 2.4% and TN from 0.02% to 0.15%. High concentrations of C_{org} and TN occur at the core

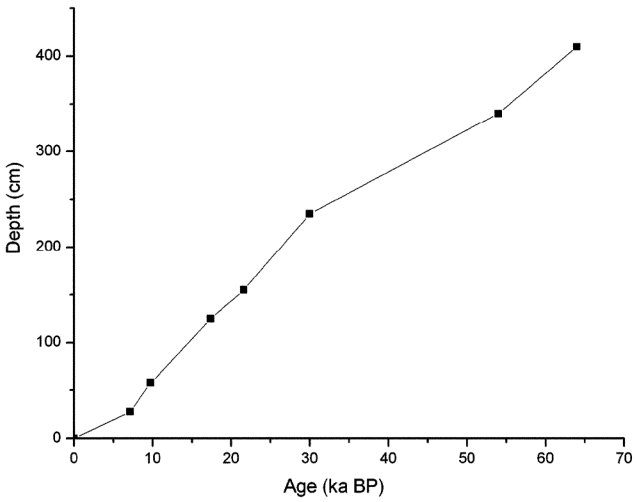

Figure 2. Age-depth profile for core SK126/39. The age model is based on calibrated ^{14}C dates (top 5 points) and downcore variations in $\delta^{18}O$ correlated with SPECMAP $\delta^{18}O$ curve (for rest of the points).

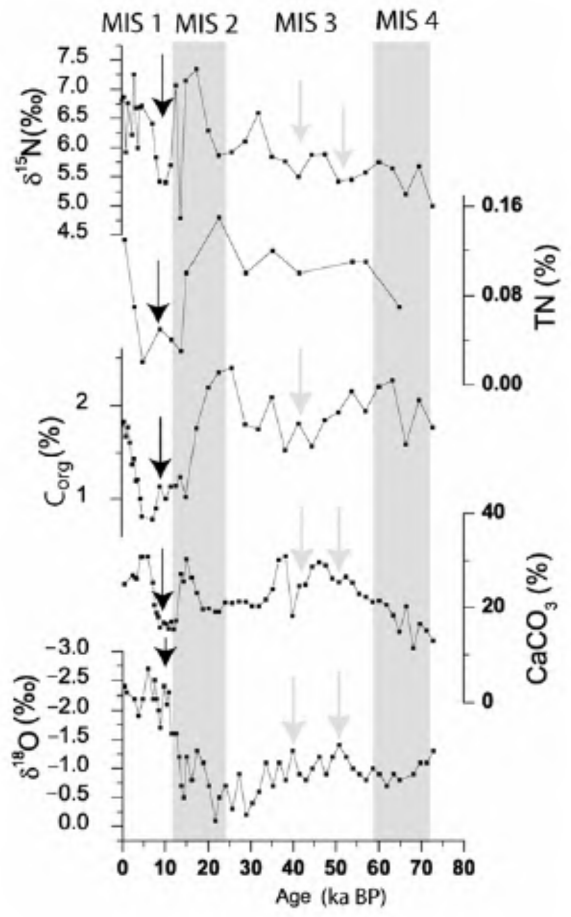

Figure 3. Stable oxygen isotope ($\delta^{18}O$) values and content of $CaCO_3$, organic carbon (C_{org}), total nitrogen (TN), and nitrogen isotope ($\delta^{15}N$) values; marine isotope stage (MIS). Black arrows show intensified monsoon signatures during MIS 1/2 and grey arrows during MIS 3.

top and during MIS 2 and MIS 4, whereas low C_{org} content characterizes the MIS 1/2 and mid-MIS 3 (Figure 3).

Variations in $\delta^{15}N$

The $\delta^{15}N$ values of organic matter range between 4.8‰ and 7.3‰. The lower $\delta^{15}N$ values are associated with Last Glacial Maximum (LGM), MIS 4, at the MIS 1/2 boundary and mid-MIS 3; higher values distinguish MIS 1 and MIS 3. Generally lower $\delta^{15}N$ values correspond to lower $\delta^{18}O$ values and lower C_{org} and $CaCO_3$ contents (Figure 3), but lower $\delta^{15}N$ is associated with higher $\delta^{18}O$, higher C_{org} and lower $CaCO_3$ during LGM and MIS 4.

Discussion

$\delta^{18}O$ record and monsoonal strength

The glacial–interglacial $\Delta\delta^{18}O$ amplitude of 2.6‰ is much larger than the combined effect of the global ice volume change (1.2‰) between LGM and Holocene[23], and regional deglacial warming (0.5‰). The $\Delta\delta^{18}O$ amplitude of 2.6‰ and residual $\Delta\delta^{18}O$ of ~0.9‰ observed in the present study are the highest so far reported in the southeastern Arabian Sea[24]. Some workers have reported small or no sea surface temperature (SST) changes in the Arabian Sea[24], whereas others have observed $\Delta\delta^{18}O$ of ~2‰ (refs 10 and 24) in the eastern Arabian Sea and related it to local changes in temperature and salinity. The higher $\Delta\delta^{18}O$ observed in this area may be because of the core location being closer to the continental margin and the associated increased amount of fresh water due to precipitation and land runoff[25].

A significant shift of $\delta^{18}O$ towards a lower value (–1.1‰) at ~15 ka BP, starting around 22 ka BP may be related to deglacial warming and/or intensification of the southwest monsoon[26]. Tiwari *et al.*[27] reported lower planktonic $\delta^{18}O$ values ~18 ka BP in the equatorial Indian ocean and ascribed it to the intensification of the northeast monsoon. However, an intensification of the southwest monsoon during this period has been reported by Sirocko *et al.*[28] using geochemical and multi-tracer studies and, by Huguet *et al.*[29] using organic proxies. The shift in $\delta^{18}O$ towards higher values around 14 ka BP (Figure 3) may be related to a reduced intensity of the southwest monsoon. Tiwari *et al.*[30] reported similarly higher $\delta^{18}O$ values and attributed it to weakened southwest monsoon during the Older Dryas and connection with the North Atlantic climate. Another interruption, marked with uniform $\delta^{18}O$ values around 12 ka BP (Figure 3) suggests the Younger Dryas colder event. Although the present data have limitations in terms of sedimentation rates and temporal resolution, significant shift towards lower values (–2.4‰) around 10 ka BP (starting from 14 ka BP) suggests further strengthening of the southwest monsoon. Intensification of the monsoon has been reported to occur in two phases at 11.5 and 9.7 ka BP in the northern Arabian Sea[28]. Due to limited number of data points, the two events are not well constrained in the core.

The MIS 3 was the time of increased insolation when the South Asian summer monsoon strengthened after MIS 4[31]. The lower $\delta^{18}O$ values at MIS 3 suggest warmer climate with increased precipitation. Within MIS 3 lower $\delta^{18}O$ values at ~40 and 50 ka BP, most probably correspond to periods of the most intense southwest monsoon. Signatures of intensified monsoon during MIS 3 have been reported in the northeastern Arabian Sea using upwelling indicators[32], but not documented in oxygen isotope data or other palaeomonsoon proxies. The heavier $\delta^{18}O$ values during MIS 4 suggest cooler climate.

Relations between monsoon strength and past productivity variations

During MIS 2 and 4: The C_{org} and TN in marine sediments are derived from the water column and serve as

proxy for the surface primary productivity[33]. However, a part of C_{org} can also be contributed by land. The present core exhibits $\delta^{13}C$ values of C_{org} between $-20.8‰$ and $-19.2‰$ (unpublished data) that are typically marine, indicating a predominantly marine source of organic matter. Relatively high C_{org} and TN content in sediments during LGM and MIS 4 suggest elevated productivity (Figure 3). During MIS 2, the southwest monsoon was weaker[25] as indicated by higher $\delta^{18}O$ values and lower SST[34]. High productivity in the study region during LGM was attributed to lower SST that might have induced convective mixing and injection of nutrients to the euphotic zone[34]. Cooler surface temperatures and higher salinities have been invoked to explain higher $\delta^{18}O$ values during MIS 2, which would also favour convection in the upper water column. It is most likely that the northward-flowing low-salinity West India Coastal Current, which presently prevents convective mixing over large parts of the western Indian shelf, weakened during LGM[25]. Our results are supportive of this hypothesis[6,10]. Several other workers[25,34] reported similar conditions even further south of our study area during LGM. Higher $\delta^{18}O$ values and high C_{org} content during MIS 4 suggest that such conditions (convective mixing and high productivity) might have occurred during other glacial stages as well in the southeastern Arabian Sea.

During MIS 1 and MIS 3: Increased C_{org}, $CaCO_3$ and TN content during MIS 1 and MIS 3 also support higher productivity which is directly related to strong southwest monsoon. Low C_{org}, TN and $CaCO_3$ contents during MIS 1/2 and mid-MIS 3 (40–50 ka BP) indicate reduced productivity. The MIS 1/2 transition, however, coincides with a strong southwest monsoon (11–6 ka BP)[10,25,35], with maximum intensity at ~11 ka BP (ref. 35). Similarly, increased upwelling has been reported during mid-MIS 3 (~ 50 ka BP)[32]. Low $\delta^{18}O$ and $CaCO_3$ content observed at ~ 40 and ~ 50 ka BP (Figure 3) further support the prevalence of reduced salinity at the study site which could be due to increased precipitation/runoff. As the core is from a monsoon-induced upwelling area[36], low productivity during the times of intense monsoon is unexpected and needs explanation. We speculate that increased freshwater inputs during these periods could have led to a much stronger stratification and a thicker fresher-water lens than exists today, thus dominating the expected intensification of coastal upwelling. Strong winds associated with the monsoon might not be able to break the stratification (barrier layer effect), as happens in the Bay of Bengal today, resulting in lower productivity. Similar oligotrophic conditions were reported in the northeast and southwest Arabian Sea during MIS 1/2 (ref. 37) and related to advection of equatorial oligotrophic surface water. Naqvi and Fairbanks[38] have reported a cessation of Red Sea water during the period of deglacial monsoon intensification. It is thus likely that a large part of the Arabian Sea received more inputs of freshwater during this period and the salinity was generally lower.

Monsoon strength – denitrification variations

During MIS 2 and MIS 4: The $\delta^{15}N$ values are lower by more than 1‰ during LGM than the late Holocene, pointing to less intense denitrifying conditions in subsurface waters during LGM. Suppressed denitrification has been previously reported based on $\delta^{15}N$ measurements in cores collected from various parts of the Arabian Sea[2,4,7] and attributed to low productivity during LGM (i.e. related to weaker southwest monsoon). Implicit in this interpretation is the assumption that the oxygen concentration in subsurface waters is dominantly controlled by productivity.

The sedimentary $\delta^{15}N$ record in the present study also indicates less intense denitrification during LGM, consistent with previous results from elsewhere in the Arabian Sea, providing further support for the $\delta^{15}N$ signal to be regional. Galbraith *et al.*[39] have related reduced denitrification rates during glacial periods to greater oxygen supply to thermocline waters. Significantly, at the core site itself productivity seems to have been higher during glacial times. The likely cause for this is mentioned here – a more intense convective mixing during winter would also keep the mesopelagic layer more oxygenated, thereby suppressing denitrification. The increase in $\delta^{15}N$ values to over 7‰ from 17 to 15 ka BP (Figure 3) suggests an increase in denitrification rate. This implies a reduction of oxygen content of subsurface waters. Note that barring a single-point sharp excursion in $\delta^{15}N$ (discussed here), there is a broad maximum in $\delta^{18}O$ that is associated with decreasing C_{org} and TN but increasing $CaCO_3$ before consistent minima in all proxies are observed around the transition from MIS 2 to MIS 1. A local intensification of the oxygen minimum during deglaciation might arise from a relaxation of convective mixing as a consequence of warming and/or change in circulation (intensification of the northward West Indian Coastal Current). Sediment cores from the southwestern Indian margin and terrestrial records do indicate warming of the climate during this period[40]. The sharp minimum in $\delta^{15}N$ to 4.8‰ around 14 ka BP (Figure 3), associated with the higher $\delta^{18}O$ values suggest a brief period of cooler climate. Similar lower $\delta^{15}N$ values have been reported by Suthhof *et al.*[13] from the northern Arabian Sea during Heinrich Events and Younger Dryas and related to the reduced denitrification and productivity. A relaxation in denitrification has been postulated to occur during each such event due to advection of more oxygenated water masses from the south into the Arabian Sea OMZ[11–13]. The low $\delta^{15}N$ values and higher C_{org} during MIS 4 suggest suppressed denitrification as a result of deep convective mixing, similar to MIS 2.

During MIS 1 and MIS 3: The fluctuations in $\delta^{15}N$ are more conspicuous during MIS 1. Reduced denitrification rates, represented by lower $\delta^{15}N$ values (to 5.4‰), correspond to lower C_{org}, TN and $CaCO_3$ contents (Figure 3) around 10 ka BP. This period of seemingly weaker denitrification coincides with intensification of the southwest monsoon[35] and increased precipitation[41]. Elsewhere in the Arabian Sea, this period is distinguished by high sedimentary $\delta^{15}N$ (refs 7 and 13). At present, the southeastern Arabian Sea is characterized by complex hydrography and biogeochemistry. Coastal upwelling stimulates phytoplankton growth and the ensuing increase in subsurface oxygen demand leads to the development of anoxic conditions over the inner- and mid-shelf regions during the late southwest monsoon[3]. This process is helped by the existence of strong near-surface stratification, as the cold, saline upwelled waters are overlain by a thin (5–10 m) warm, low-salinity cap. However, off the continental margin of India, the presence of the undercurrent, a part of the SW monsoon circulation, prevents the development of suboxic conditions. The lighter $\delta^{15}N$ observed during the intensified monsoon[35], could again be a local feature arising from a more vigorous undercurrent during the southwest monsoon. At the same time, it is also possible that there was greater intrusion of nutrient-poor, surface water from the south as proposed by Rixen *et al.*[42].

Higher denitrification rates since 7 ka BP are suggested by relatively high $\delta^{15}N$ values (~6.7‰) and are largely similar to that of the present day, except at ~4, ~2.5 and ~1 ka BP (Figure 3). Overall, there does not seem to have been any major fluctuation in subsurface oxygen distribution. Lower $\delta^{15}N$ value around 4 ka BP indicates reduced denitrification that seems to be associated with a weaker southwest monsoon. However, it must be pointed out that the core examined here exhibits relatively low sedimentation rates that could have dampened the signal and prevented resolution of high frequency changes. Cores along the continental shelf/upper slope of India with higher sedimentation rates may provide a better insight into these variations.

As indicated earlier, MIS 3 was a time of generally higher insolation, and strengthened SW monsoon[31]. However, large changes in sedimentary $\delta^{15}N$ values have been reported during this stage that seem to relate well to climate variability in the North Atlantic as recorded in the sediments and Greenland ice cores with warm (cold) events in the North Atlantic corresponding to high (low) $\delta^{15}N$ in the Arabian Sea sediments[7,13]. In our core, variations in $\delta^{15}N$ values during MIS 3 are smaller compared to MIS 1, but this could well be due to coarser temporal resolution. Nevertheless, denitrification seems to have been weaker around 40 and 50 ka BP, again associated with the intensification of SW monsoon within MIS 3.

1. Naqvi, W. A., Geographical extent of denitrification in the Arabian Sea in relation to some physical processes. *Oceanol. Acta.*, 1991, **14**, 281–290.
2. Ganeshram, R. S., Pedersen, T. F., Calvert, S. E., McNeill, G. W. and Fontugne, M. R., Glacial–intergalcial variability in denitrification in the world's oceans: causes and consequences. *Paleoceanography*, 2000, **14**, 361–376.
3. Naqvi, S. W. A. *et al.*, Budgetary and biogeochemical implications of N_2O isotope signatures in the Arabian Sea. *Nature*, 1998, **394**, 462–464.
4. Altabet, M. A., Murray, D. W. and Prell, W. L., Climatically linked oscillations in Arabian Sea denitrification over the past 1 m.y.: implications for the marine N cycle. *Paleoceanography*, 1999, **4**, 732–743.
5. Agnihotri, R., Bhattacharya, S. K., Sarin, M. M. and Somayajulu, B. L. K., Changes in surface productivity and subsurface denitrification during the Holocene: a multiproxy study from the eastern Arabian Sea. *The Holocene*, 2003, **13**, 701–713.
6. Banakar, V. K., Oba, T., Chodankar, A. R., Kuramoto, T. and Minagawa, M., Monsoon related changes in sea surface productivity and water column denitrification in the eastern Arabian Sea during the last glacial cycle. *Mar. Geol.*, 2005, **219**, 99–108.
7. Altabet, M. A., Higginson, M. J. and Murray, D. W., The effect of millennial-scale changes in Arabian Sea denitrification on atmospheric CO_2. *Nature*, 2002, **415**, 159–162.
8. Reichart, G. J., Lourens, L. J. and Zachariasse, W. J., Temporal variability in the northern Arabian Sea Oxygen Minimum Zone (OMZ) during the last 225,000 years. *Paleoceanography*, 1998, **13**, 319–321.
9. Naidu, A. S. and Shankar, R., Palaeomonsoon history during the last Quaternary: results of a pilot study on sediments from the Laccadive trough, Southeastern Arabian Sea. *J. Geol. Soc. India*, 1999, **53**, 401–406.
10. Thamban, M., Rao, V. P., Schneider, R. R. and Grootes, P. M., Glacial to Holocene fluctuations in hydrography and productivity along the southwestern continental margin of India. *Palaeogeogr. Palaeoclimatol. Palaeoecol.*, 2001, **165**, 113–127.
11. Gupta, A. K., Das, M., Clemens, S. C. and Mukherjee, B., Benthic foraminiferal faunal and isotopic changes as recorded in Holocene sediments of the northwest Indian Ocean. *Paleoceanography*, 2008, **23**, doi:10.1029/2007PA001546.
12. Schmiedl, G. and Leuschner, D. C., Oxygenation changes in the deep water Arabian Sea during the last 190,000 years: productivity versus deepwater circulation. *Paleoceanography*, 2005, **20**, doi:10.1029/2004PA001044.
13. Suthhof, A., Ittekkot, V. and Gaye-Haake, B., Millennial-scale oscillations of denitrification intensity in the Arabian Sea during the late Quaternary and its potential influence on atmospheric N_2O and global climate. *Glob. Biogeochem. Cycles*, 2001, **15**, 637–650.
14. Qasim, S. Z., Biological productivity of the Indian Ocean. *Indian J. Mar. Sci.*, 1977, **6**, 122–137.
15. Wyrtki, K., *Oceanographic Atlas of International Indian Ocean Expedition*, National Science Foundation, Washington DC, 1971, p. 531.
16. Sen Gupta, R. and Naqvi, S. W. A., Chemical oceanography of the Indian Ocean, north of the equator. *Deep-Sea Res.*, 1984, **31**, 671–706.
17. Naqvi, S. W. A., Naik, H. and Narvekar, P. V., The Arabian Sea. In *Biogeochemistry of Marine Systems* (eds Black, K. and Shimmield, G. B.), Oxford, UK, 2003, pp. 157–207.
18. Chivas, A. R., De Deckker, P., Wang, S. X. and Cali, J. A., Oxygen isotope systematics of the nektic ostracod *Australocypris robusta*. The Ostracoda: applications in Quaternary research. *Am. Geophys. Union, Geophys. Monogr.*, 2002, **131**, 301–313.
19. Kessarkar, P., Investigation on the sediment cores of the Bengal Fan: inferences on the provenance of sediments during the late Quaternary, Ph D thesis, Goa University, Goa, India, 2004, p. 199.
20. Stuiver, M., Reimer, P. J. and Braziunas, T. F., High-precision radiocarbon age calibration for terrestrial and marine samples. *Radiocarbon*, 1998, **40**, 1127–1151.

21. Imbrie, J. *et al.*, The orbital theory of Pleistocene climate: support from a revised chronology of the marine $\delta^{18}O$ record. In *Milankovitch and Climate, Part I* (eds Berger, A. L. *et al.*), Reidel, Dordrecht, 1984, pp. 269–305.
22. Bassinot, F. C., Labeyrie, L. D., Vincent, E., Quidelleur, X., Shackleton, N. J. and Lancelot, Y., The astronomical theory of climate and the age of the Brunhes–Matuyama magnetic reversal. *Earth Planet. Sci. Lett.*, 1994, **126**, 91–108.
23. Fairbanks, R., A 17,000 year glacio-eustatic sea level record: influence of glacial melting rates on the Younger Dryas event and deep-ocean circulation. *Nature*, 1989, **342**, 637–642.
24. Prabhu, C. N., Shankar, R., Anupama, K., Taieb, M., Bonnefille, R., Vidal, L. and Prasad, S., A 200-ka pollen and oxygen isotopic record from two sediment cores from the eastern Arabian Sea. *Palaeogeogr. Palaeoclimatol. Palaeoecol.*, 2004, **214**, 309–321.
25. Duplessy, J. C., Glacial to interglacial contrasts in the northern Indian Ocean. *Nature*, 1982, **295**, 494–498.
26. Ahmad, M. S., Babu, A. G., Padmakumari, V. M. and Raza, W., Surface and deep water changes in the northeast Indian Ocean during the last 60 ka inferred from carbon and oxygen isotopes of planktonic and benthic foraminifera. *Palaeogeogr. Palaeoclimatol. Palaeoecol.*, 2008, **262**, 182–188.
27. Tiwari, M., Ramesh, R., Somayajulu, B. L. K., Jull, A. J. T. and Burr, G. S., Early deglacial (~19–17 ka) strengthening of the northeast monsoon. *Geophys. Res. Lett.*, 2005, **32**, doi:10.1029/2005GL024070.
28. Sirocko, F., Schonberg, D. G. and Devey, C., Processes controlling trace element geochemistry of Arabian Sea sediments during the last 25,000 years. *Glob. Planet. Change*, 2000, **26**, 217–303.
29. Huguet, C., Kim, J.-H., Damsté, J. S. S. and Scjpitem, S., Reconstruction of sea surface temperature variations in the Arabian Sea over the last 23 kyr using organic proxies (TEX_{86} and $U^{K'}_{37}$). *Paleoceanography*, 2006, **21**, PA30003.
30. Tiwari, M., Ramesh, R., Somayajulu, B. L. K., Jull, A. J. T. and Burr, G. S., Paleomonsoon precipitation deduced from a sediment core from the equatorial Indian Ocean. *Geo-Mar. Lett.*, 2006, **26**, 23–30.
31. Owen, L. A., Finkel, R. C. and Caffee, M. W., A note on the extent of glaciation throughout the Himalaya during the global Last Glacial Maximum. *Quat. Sci. Rev.*, 2002, **21**, 147–157.
32. Leuschner, D. C. and Sirocko, F., Orbital insolation forcing of the Indian monsoon – a motor for global climate changes? *Palaeogeogr. Palaeoclimatol. Palaeoecol.*, 2003, **197**, 83–95.
33. Muller, P. J. and Suess, E., Productivity, sedimentation rate, and sedimentary organic matter in the oceans-I. Organic carbon preservation. *Deep Sea Res.*, 1979, **26A**, 1347–1362.
34. Rostek, F., Bard, E., Beaufort, L., Sonzogni, C. and Ganssen, G., Sea surface temperature and productivity records for the past 240 kyr in the Arabian Sea. *Deep-Sea Res.*, 1997, **44**, 1461–1480.
35. van Campo, E., Monsoon fluctuations in 20,000 yr BP oxygen-isotope/pollen records of southwest India. *Quat. Res.*, 1986, **26**, 376–388.
36. Shetye, S. R., Gouveia, A. D., Shenoi, S. S. C., Sunder, D., Michael, G. S., Almeida, A. M. and Santanam, K., Hydrography and circulation off the west coast of India during the southwest monsoon 1987. *J. Mar. Res.*, 1990, **48**, 359–378.
37. Rogalla, U. and Anruleit, H., Precessional forcing and coccolithophore assemblages in the northern Arabian Sea: implications for monsoonal dynamics during the last 200,000 years. *Mar. Geol.*, 2005, **217**, 31–48.
38. Naqvi, W. A. and Fairbanks, R. G., A 27,000 year record of Red Sea outflow: implication for timing of post-glacial monsoon intensification. *Geophys. Res. Lett.*, 1996, **23**, 1501–1504.
39. Galbraith, E. D., Kienast, M., Pedersen, T. F. and Calvert, S. E., Glacial–interglacial modulation of the marine nitrogen cycle by high-latitude O_2 supply to the global thermocline. *Paleoceanography*, 2004, **19**, PA4007.
40. Sukumar, R., Ramesh, R., Pant, R. K. and Rajagopalan, G., A $\delta^{13}C$ record of late Quaternary climate change from tropical peats in southern India. *Nature*, 1993, **364**, 703–706.
41. Sarkar, A., Ramesh, R., Bhattacharya, S. K. and Price, N. B., Palaeomonsoon and palaeoproductivity records of $\delta^{18}O$, $\delta^{13}C$ and $CaCO_3$ variations in the northern Indian Ocean sediments. *Proc. Indian Acad. Sci.: Earth Planet. Sci.*, 2000, **109**, 157–169.
42. Rixen, T., Haake, B., Ittekkot, V., Guptha, M. V. S., Nair, R. R., and Schlussel, P., Coupling between SW monsoon-related surface and deep ocean processes as discerned from continuous particle flux measurements and correlated satellite data. *J. Geophys. Res.*, 1996, **101**, 28569–28582.

ACKNOWLEDGEMENTS. We thank the Director, National Institute of Oceanography, Goa, for facilities and encouragement. Part of the work was done under the 'Young Scientist Project' awarded to P.M.K. by the Department of Science and Technology, New Delhi. We thank Dr C. Prakash Babu for the help in C, N elemental analysis. Ms Supriya Karapurkar is acknowledged for her help in isotopic measurements. This is NIO contribution number 4809.

Received 30 April 2009; revised accepted 13 July 2010